Since January 2020 Elsevier has created a COVID-19 resource centre with free information in English and Mandarin on the novel coronavirus COVID-19. The COVID-19 resource centre is hosted on Elsevier Connect, the company's public news and information website.

Chemico-Biological Interactions 365 (2022) 110097

Contents lists available at ScienceDirect

Chemico-Biological Interactions

journal homepage: www.elsevier.com/locate/chembioint

Research paper

In vitro evaluation of the impact of Covid-19 therapeutic agents on the hydrolysis of the antiviral prodrug remdesivir

Qingchen Zhang [a], Philip W. Melchert [a], John S. Markowitz [a,b,*]

[a] Department of Pharmacotherapy and Translational Research, Gainesville, FL, USA
[b] Center for Pharmacogenomics and Precision Medicine, University of Florida, Gainesville, FL, USA

ARTICLE INFO

Keywords:
Remdesivir
Cannabidiol
CES1
G143E
COVID-19

ABSTRACT

Remdesivir (RDV, Veklury®) is an FDA-approved prodrug for the treatment of hospitalized patients with COVID-19. Recent in vitro studies have indicated that human carboxylesterase 1 (CES1) is the major metabolic enzyme catalyzing RDV activation. COVID-19 treatment for hospitalized patients typically also involves a number of antibiotics and anti-inflammatory drugs. Further, individuals who are carriers of a *CES1* variant (polymorphism in exon 4 codon 143 [G143E]) may experience impairment in their ability to metabolize therapeutic agents which are CES1 substrates. The present study assessed the potential influence of nine therapeutic agents (hydroxychloroquine, ivermectin, erythromycin, clarithromycin, roxithromycin, trimethoprim, ciprofloxacin, vancomycin, and dexamethasone) commonly used in treating COVID-19 and 5 known CES1 inhibitors on the metabolism of RDV. Additionally, we further analyzed the mechanism of inhibition of cannabidiol (CBD), as well as the impact of the G143E polymorphism on RDV metabolism. An in vitro S9 fraction incubation method and in vitro to in vivo pharmacokinetic scaling were utilized. None of the nine therapeutic agents evaluated produced significant inhibition of RDV hydrolysis; CBD was found to inhibit RDV hydrolysis by a mixed type of competitive and noncompetitive partial inhibition mechanism. In vitro to in vivo modeling suggested a possible reduction of RDV clearance and increase of AUC when coadministration with CBD. The same scaling method also suggested a potentially lower clearance and higher AUC in the presence of the G143E variant. In conclusion, a potential CES1-mediated DDI between RDV and the nine assessed medications appears unlikely. However, a potential CES1-mediated DDI between RDV and CBD may be possible with sufficient exposure to the cannabinoid. Patients carrying the *CES1* G143E variant may exhibit a slower biotransformation and clearance of RDV. Further clinical studies would be required to evaluate and characterize the clinical significance of a CBD-RDV interaction.

1. Introduction

Remdesivir (RDV, Veklury®) is a SARS-CoV-2 nucleotide analog RNA polymerase inhibitor [1] and the first FDA-approved antiviral to treat COVID-19 [2]. Intravenous remdesivir is approved by the Food and Drug Administration (FDA) for the treatment of mild to moderate COVID-19 in high-risk, nonhospitalized patients and for the treatment of hospitalized patients with COVID-19. Following intravenous administration, the major portion (>90%) of this prodrug is rapidly hydrolyzed to the intermediate metabolite GS-704277 by liver esterases, with a small portion of the drug (7.4%–9.9%) eliminated unchanged [3]. GS-704277 is then further metabolized by intracellular phosphoramides and phosphotransferases to its active form, GS-441524 [4]. Recent in vitro studies have indicated that carboxylesterase 1 (CES1) is the major drug-metabolizing enzyme (DME) catalyzing the initial hydrolyzing step of RDV metabolism with an additional contribution from cathepsin A (CatA) [5] (Fig. 1).

Drug-drug interactions (DDIs), as well as the presence of genetic variants of DMEs, can compromise drug therapy. Importantly, beyond antiviral treatment, patients hospitalized for COVID-19 typically receive a number of concomitant medications including off-label antivirals, antibiotics, anti-inflammatories, and others [6]. Many of these co-administered agents have documented effects on DMEs such as CYP3A [7,8], but few have undergone assessment for their potential influence on CES1, and accordingly, RDV metabolism. The present study utilized previously established in vitro methods [9] to assess the potential influence of nine therapeutic agents frequently utilized in the

* Corresponding author. Department of Pharmacotherapy and Translational Research University of Florida, College of Pharmacy 11600 SW Archer Road, RM PG 4-31, Gainesville, FL, 32610-0486, USA.
E-mail address: jmarkowitz@cop.ufl.edu (J.S. Markowitz).

https://doi.org/10.1016/j.cbi.2022.110097
Received 16 June 2022; Received in revised form 1 August 2022; Accepted 6 August 2022
Available online 11 August 2022

Abbreviations

RDV	Remdesivir
CES1	Human carboxylesterase 1
G143E	CES1 polymorphism in exon 4 codon 143
CBD	Cannabidiol
FDA	The Food and Drug Administration
DME	Major drug-metabolizing enzyme
CatA	Cathepsin A
DDIs	Drug-drug interactions
THC	Δ9-tetrahydrocannabinol
CBN	Cannabinol
IS	Internal standard
[S]	Substrate concentration
V	Reaction velocity
Km	Substrate concentration at half of the maximum reaction velocity
Vmax	Maximum reaction velocity
[I]	Inhibitor concentration
Rv	The ratio of reaction velocity with coadministration of inhibitor divided by reaction velocity in the control condition without inhibitor, expressed as percent
γ	Exponent in the Hill equation
IC	Inhibitor concentration producing 50% of maximum inhibition
Emax	Maximum effect
E0	Baseline effect
[I]	The inhibitor concentration
Ki	Inhibition constant
α	The mix of non-competitive and competitive inhibition
β	The ratio of remaining enzyme velocity when bound to the inhibitor
AUC_i	Area under the curve of victim drug with the presence of the inhibitor
AUC_o	Area under the curve of the victim drug in absence of the inhibitor
$CL_{int,\ i}$	Intrinsic clearance by CES1 of the victim drug with the presence of the inhibitor
$CL_{int,\ o}$	Intrinsic clearance by CES1 of the victim drug in absence of the inhibitor
fm	Fraction of metabolism
CL_i	Clearance of the victim drug in presence of the inhibitor
CL_o	Clearance of the victim drug in absence of the inhibitor
R_{AUC}	Predicted change in the substrate drug AUC
R_{CL}	Predicted change in the substrate drug clearance
MAF	Minor allele frequency

treatment of COVID-19 and its complications on the initial hydrolysis of RDV. Agents chosen for the evaluation of CES1 inhibitory activity included hydroxychloroquine, ivermectin, erythromycin, clarithromycin, roxithromycin, trimethoprim, ciprofloxacin, vancomycin, and dexamethasone. Additionally, due to the increasing use of medical cannabis and cannabidiol (CBD) supplements, their advocacy for certain COVID-19 associated conditions [10,11] and emerging evidence of CES1 inhibition by the major cannabinoids [12], Δ^9-tetrahydrocannabinol (THC), CBD, and cannabinol (CBN) were evaluated (Table 1). In addition, since individuals who are carriers of the loss of function *CES1* variant G143E have a demonstrated impairment in their ability to metabolize CES1 substrates [13–15], influences of the variant on the hydrolysis of RDV were evaluated as well. An established cell-line and in vitro assay was also utilized to investigate the influence of the variant on the conversion of RDV to GS-704277 [16]. Finally, a mathematical model was applied to evaluate the pharmacokinetic change due to the reduction of CES1 activity. This model was applied to our in vitro data to quantitively evaluate the impact of the coadministration of RDV with the respective inhibitor from the screening result, as well as individuals with the G143E variant.

2. Methods and materials

2.1. Materials

Remdesivir (RDV), GS704277, THC, CBD, CBN, hydroxychloroquine were purchased from Cayman Chemical (Ann Arbor, MI). Azithromycin was purchased from Pfizer Inc. (New York NY). Erythromycin,

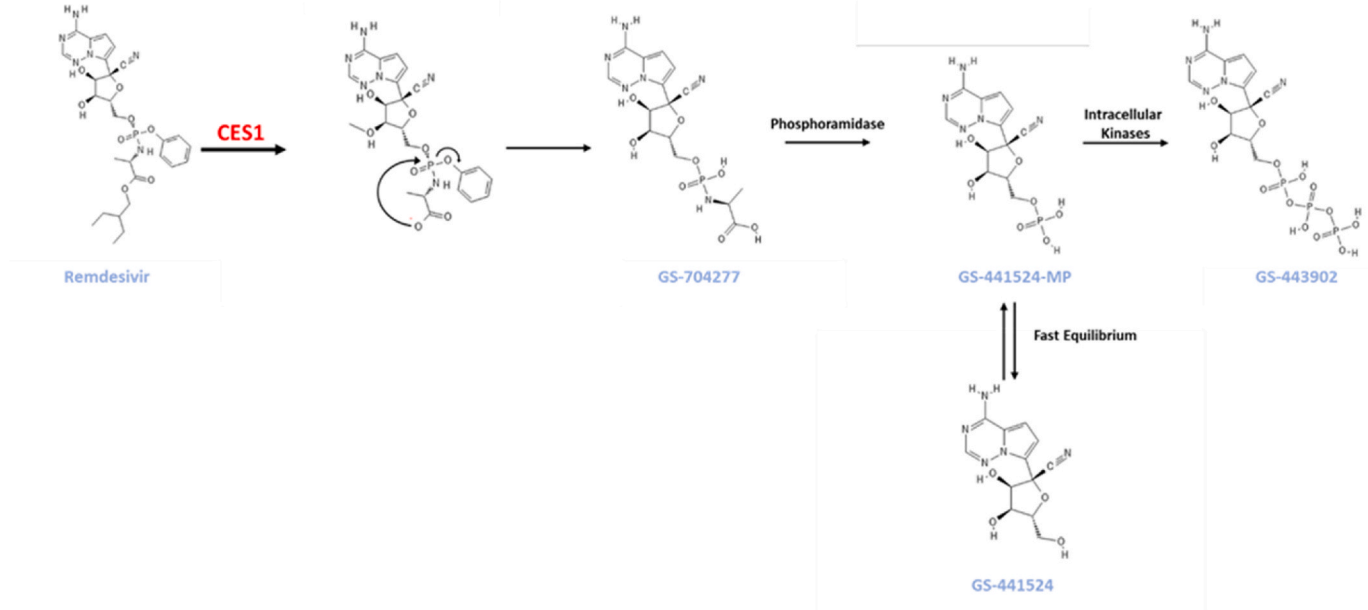

Fig. 1. Metabolic pathway of RDV.

Table 1
In vivo concentration ranges of the study compounds.

Name of compound	Molecular weight	Concentration use in this study		In vivo Cmax		Dose	Subjects	N	Reference
	g/mol	μg/mL	μM	μg/mL	μM				
Aripiprazole	448.39	10.00	22.30	0.14	0.31	P.O. 10 mg/day tablets	Healthy subjects	24	[17]
Ziprasidone	412.94	10.00	24.22	0.09	0.22	P.O. 40 mg tablets	Healthy subjects	10	[18]
CBN	310.43	10.00	32.21	0.01	0.02	Case report	–	–	[19]
THC	314.45	10.00	31.80	1.10	3.50	Case report	–	–	[19]
CBD	314.47	10.00	31.80	1.39	4.40	P.O. 1500 mg CBD twice daily	Healthy subjects	9	[20]
Dexamethasone	392.46	10.00	25.48	0.26	0.66	P.O. 20 mg tablet under fasting conditions	Healthy subjects	34	[21]
Trimethoprim	290.32	10.00	34.44	2.70	9.30	P.O. 400:2000 mg trimethoprim: sulfamethoxazole	Healthy subjects	24	[22]
Ivermectin	875.10	10.00	11.43	0.08	0.09	P.O. 12 mg solution	Healthy subjects	11	[23]
Azithromycin	749.00	10.00	13.35	0.40	0.53	P.O. 500 mg	Healthy subjects	12	[24,25]
Clarithromycin	747.95	10.00	13.37	2.85	3.81	P.O. 500 mg	Healthy subjects	17	[26]
Ciprofloxacin	331.35	10.00	30.18	1.10	3.32	P.O. 200 mg	Healthy subjects	12	[27]
Erythromycin	733.93	10.00	13.63	3.49	4.75	P.O. 800 mg every 12 h for 3 doses	Healthy subjects	23	[28]
Roxithromycin	837.05	10.00	11.95	9.70	11.59	P.O. 300 mg	Healthy subjects	20	[29]
Vancomycin	1449.30	10.00	6.90	10.00	6.90	I.V. 10 mg/kg	Patients	6	[30]
Hydroxychloroquine	335.87	10.00	29.77	3.30	9.83	I.V. 310 mg over 0.5 h	Healthy subjects	4	[31]

clarithromycin was purchased from Abbott Laboratories Inc. (Chicago, IL). Dexamethasone, trimethoprim, ivermectin ciprofloxacin, roxithromycin, vancomycin, aripiprazole, ziprasidone, and phenacetin were purchased from Sigma-Aldrich Inc. (St. Louis, MO). Phosphate buffered saline (PBS) was purchased from Thermo Fisher Scientific Inc. (Waltham, MA). All other chemicals and reagents were of the highest analytical grade and were commercially available.

2.2. Preparation of cell S9 fractions containing wild-type CES1

Wild-type and G143E S9 fractions were prepared as previously described [13]. In brief, human embryonic kidney cell line (Flp-In-293, Invitrogen, Carlsbad, CA) stably expressing WT and *CES1* G143E [13] were cultured in Dulbecco's modified Eagle medium with 10% FBS and 100 mg/ml hygromycin. Upon reaching approximately 90% confluency, cells were then harvested in PBS and sonicated for 10 s. The mixture was then centrifuged at 9000 g for 30 min to isolate the S9 fraction which was then stored at −70 °C until use. The total protein concentrations in S9 fractions were determined using a Pierce BCA Protein Assay Kit (Thermo Fisher Scientific Inc.).

2.3. General in vitro assay conditions

Stock solutions of RDV and the agents assessed for inhibition were made in DMSO at a concentration of 20 mM. Prior to experiments, RDV and prospective inhibitors were prediluted with PBS into an intermediate concentration and further diluted into 96-well plates in a series of concentrations (7.8, 15.6, 31.2, 62.5, 125, 250 μM). The S9 fractions were diluted in PBS and maintained on ice during the experimental workup. In addition to the substrate (RDV) and prospective inhibitors, the mixture contains 40 μg/ml of S9 fraction for a total volume of 100 μl. The reaction was initiated by the addition of the S9 fraction and terminated by the addition of 30 μl of 100 μM phenacetin (internal standard; IS) in acetonitrile. Ninety-six well plates were kept in a water bath maintained at 37 °C. The incubation time was determined in the linear phase of the metabolite formation vs the incubation time curve determined in our preliminary experiments and was chosen to be 45 min. After the reaction was terminated, samples were then centrifuged at 3486 g for 10 min to separate the protein, and the supernatant was collected and analyzed for RDV, GS704277 and IS. The analysis was achieved utilizing an 1100 series Agilent HPLC with Diode Array Detector (Agilent Technologies, Palo Alto, USA). Agilent Openlab software was used for data acquisition and analysis (Santa Clara, CA). A gradient method was utilized based on a previously published method with minor modifications [32]. Briefly, the mobile phase was initiated with 98% 5 mM (pH = 4) KH_2PO_4 buffer balanced with methanol and kept for 0.2 min, then the gradient changed to 10% buffer at 10 min. The ratio was then held for 1 min, and switched back to the 98% buffer for 0.5 min, balanced for another 3.5 min for a total run time of 15 min. A Synergi™ 4 μm Max-RP 80 Å, 100 × 4.6 mm LC column (Phenomenex, Torrance, CA, USA) was utilized for analysis. The UV absorbance was set at 240 nm. The concentration of GS-704277 was determined by the peak area ratio of the GS704277 and the IS phenacetin, and was compared with a standard curve. Representative chromatographic peaks are shown in Fig. 2.

2.4. Determination of in vitro inhibition prospective to the RDV metabolism

The screening of the candidate CES1 inhibitor drugs was performed by co-incubating RDV with 10 μg/mL of each drug and comparing it with a control in which no prospective inhibitor was added. The conversion of 10 μg/ml to the respective molar concentration units are provided in Table 1.

The IC50 of the potential inhibitors from the screen results was measured by coincubation of varying concentrations of inhibitors incubated with 40 μM RDV and compared with a control.

To determine if the potential inhibitor produced time-dependent inhibition, the S9 fraction and inhibitor were co-incubated for 30 min before the addition of RDV, and the result was compared with a control group in which the S9 fraction was exposed to substrate and inhibitor immediately.

To investigate the kinetic inhibition mechanism and calculated inhibition constant (Ki), various concentrations of RDV (7.8, 15.6, 31.2, 62.5, 125 μM) co-incubated with varying concentrations of CBD (0, 0.78, 1.56, 3.13, 6.25, 12.5 μM). All incubations were performed in duplicate.

2.5. Statistical analysis

Models were fitted to the data points by nonlinear regression using GraphPad PRISM 9 (San Diego, CA). Basic models were used as previously described [33]. The fundamental kinetic model utilized was the Michaelis-Menten model [34]:

$$V = \frac{Vmax[S]}{Km + [S]} \quad (1)$$

Data points are: [S]: substrate concentration, and V: reaction velocity. Iterated variables are: Km: substrate concentration at half of the maximum reaction velocity, and Vmax: maximum reaction velocity.

The kinetic model for determination of the IC50 was the Hill Equation with modification (Eq. (2)) [35]. The derivation of the equation to

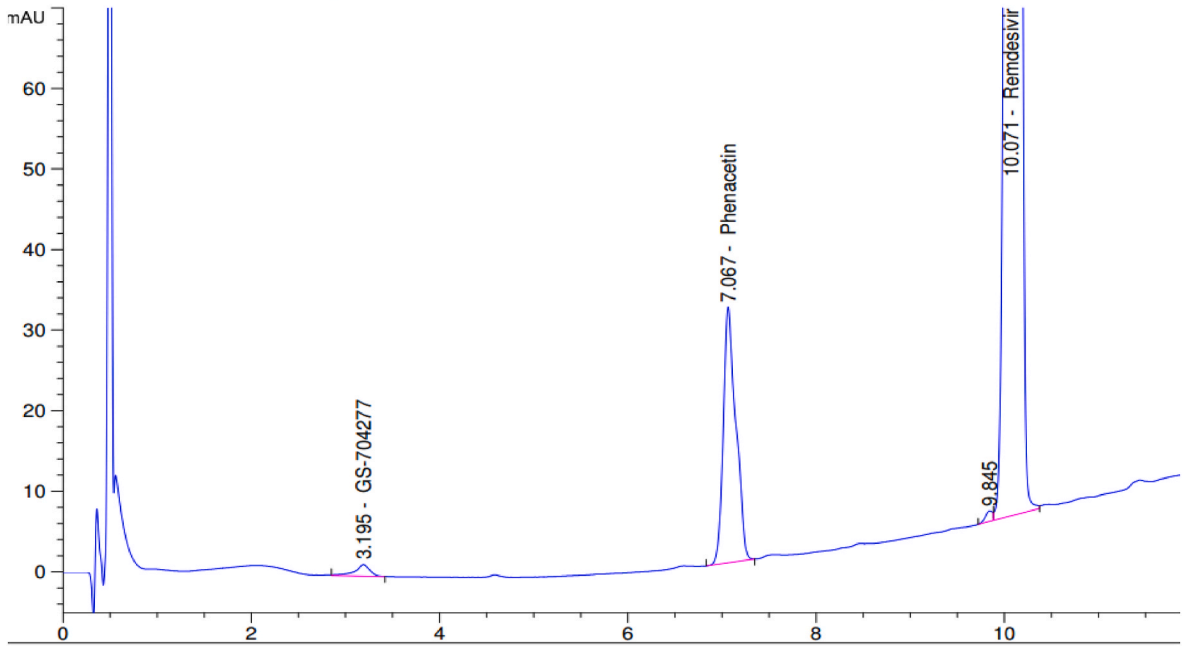

Fig. 2. Chromatograph of GS-704277, the IS phenacetin, and RDV. The standard solution was made with 6.25 μM GS704277 and 625 μM RDV in water mixed with 3:1 (v/v) 100 μM phenacetin in acetonitrile as the internal standard.

calculate IC50 (Eq. (3)) has been described previously [36], which was derived by setting the left side of Eq. (2) to be 50. The substrate concentration is fixed and chosen to be close to the substrate Km.

$$Rv = E0^{*}\left(1 - \frac{Emax[I]^{\gamma}}{[I]^{\gamma} + IC^{\gamma}}\right) \tag{2}$$

$$IC50 = \frac{IC}{\left(\frac{E0}{E0-50}{}^{*}Emax - 1\right)^{1/\gamma}} \tag{3}$$

Data points are: [I]: inhibitor concentration, and Rv: the ratio of reaction velocity with coadministration of inhibitor divided by reaction velocity in the control condition without inhibitor, expressed as percent. Iterated variables are: γ: exponent in the Hill equation, IC: inhibitor concentration producing 50% of maximum inhibition, Emax: maximum effect, E0: Baseline effect. The true IC50 is calculated from Equation (3) based on the iterated variables from nonlinear regression.

A mixed-type partial inhibition model [33] was used to determine Ki, a, and b (Equation (4)).

$$V = \frac{Vmax[S]}{Km\frac{\left(1+\frac{[I]}{Ki}\right)}{\left(1+\frac{\beta^{*}[I]}{Ki}\right)} + [S]\frac{\left(1+\frac{[I]}{\alpha^{*}Ki}\right)}{\left(1+\frac{\beta^{*}[I]}{\alpha^{*}Ki}\right)}} \tag{4}$$

Data points are: [S], substrate concentration depending on the experiments, and [I], the inhibitor concentration. Iterated variables are: Ki: inhibition constant, α: the mix of non-competitive and competitive inhibition, β: the ratio of remaining enzyme velocity when bound to the inhibitor.

The risk of coadministration of RDV and CBD was evaluated with an FDA-suggested model for DDI [37,38] with the modification to the mix-type partial model (Equation (5)) [39]. Without a suggested dose of using CBD in COVID-19 treatment available, we chose the maximum plasma concentration of approved oral CBD administration from a previously reported PK study [20] to estimate a "worst-case scenario" of high systemic exposure. Other parameters incorporated into the model were either from this in vitro enzyme kinetic experiment or from previously published literature, the details of which are listed in Table 1.

$$\frac{AUC_i}{AUC_o} = \frac{CL_o}{CL_i} = \frac{1}{fm^{*}\frac{CL_{int,i}}{CL_{int,o}} + (1-fm)} = \frac{1}{fm^{*}\frac{ki+\frac{b}{a}^{*}[I]}{ki+[I]} + (1-fm)} \tag{5}$$

Iterated variables: AUC_i: Area under the curve of victim drug with the presence of the inhibitor; AUC_o: Area under the curve of the victim drug in absence of the inhibitor; $CL_{int,\ i}$: Intrinsic clearance by CES1 of the victim drug with the presence of the inhibitor; $CL_{int,\ o}$: Intrinsic clearance by CES1 of the victim drug in absence of the inhibitor; fm: fraction metabolism; CL_i: Clearance of the victim drug in presence of the inhibitor; CL_o: clearance of the victim drug in absence of the inhibitor. Predicted change in the substrate drug AUC (R_{AUC}) was calculated by AUC_i/AUC_o, predicted change in the substrate drug clearance (R_{CL}) was calculated by CL_i/CL_o Other variables are the same as previous equations.

3. Results

3.1. CES1 catalyzed RDV hydrolysis and Michaelis–Menten kinetics

The result of in vitro incubations of RDV is shown in Fig. 3 $r^2 \geq 0.95$ indicates a good fit of the Michaelis-Menten model confirming our assumptions of the mechanism of CES1 catalyzation is Michaelis-Menten kinetics. Vmax = 2.34 nmol/min/mg protein and Km = 14.19 μM is close to the result from the other group [16].

3.2. CBD exhibited the highest degree of inhibition of RDV among all evaluated compounds

The 2nd generation antipsychotic compounds aripiprazole and ziprasidone, as well as the major cannabinoids CBD, CBN, and THC have been identified as potent in vitro CES1 inhibitors in our previous research [12,40]. Of these agents, all produced a ≥50% inhibition of RDV hydrolysis. For ziprasidone and CBN, RDV metabolite formation was completely inhibited at the selected concentration (10 μg/mL). Dexamethasone, trimethoprim, ivermectin, azithromycin, clarithromycin, ciprofloxacin, erythromycin, roxithromycin, vancomycin, hydroxychloroquine, CBD were selected as co-administratered drugs to treat COVID-19 [6]. Among all the evaluated compounds, CBD produced

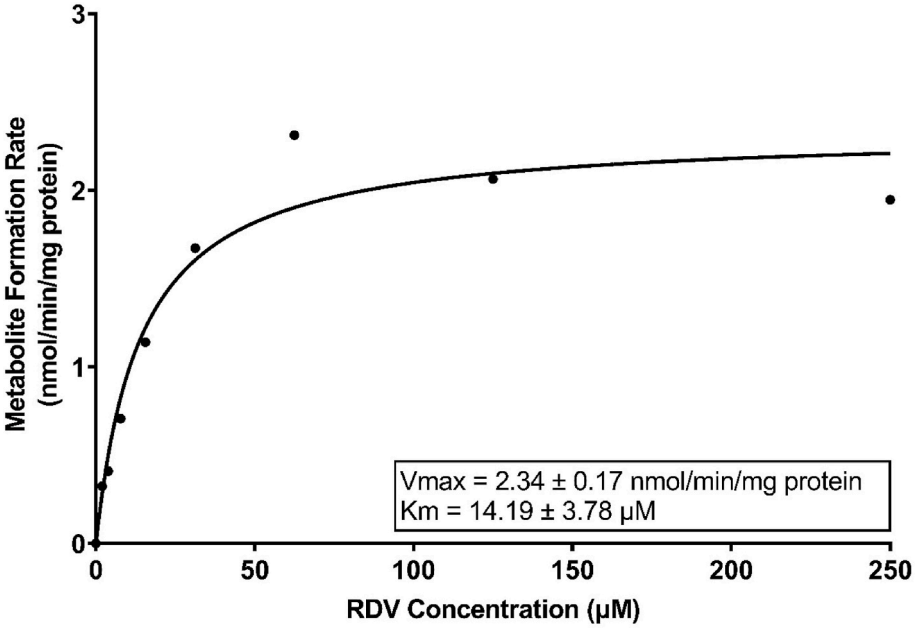

Fig. 3. S9 fraction incubation of RDV. Model: Eq. (2). $r^2 = 0.95$. Each data point was average of the duplication. Values are shown with best fit value ± SE.

the highest degree of inhibition (residual enzyme activity = ~16.5%) (Fig. 4).

3.3. Clarithromycin weakly inhibits RDV hydrolysis

Since the clarithromycin results indicated 36% residual enzyme activity, to validate this result, follow-up experiments were conducted and confirmed that clarithromycin inhibits RDV hydrolysis albeit, weakly (Fig. 5). An IC50 could not be calculated since the Emax was less than 0.5.

3.4. CBD inhibits RDV hydrolysis by reversible inhibition with an IC50 = 10.22 μM

Further preincubation results showed that at a substrate concentration of 40 μM, CBD inhibited RDV hydrolysis with an IC50 = 10.22 μM (Fig. 6). The preincubation experiment performed on the preincubation group and control group, paired by the same CBD concentration indicated a non-significant difference (P = 0.2087; paired *t*-test). This result suggests CBD inhibited RDV metabolism by a reversible inhibition mechanism (Fig. 6).

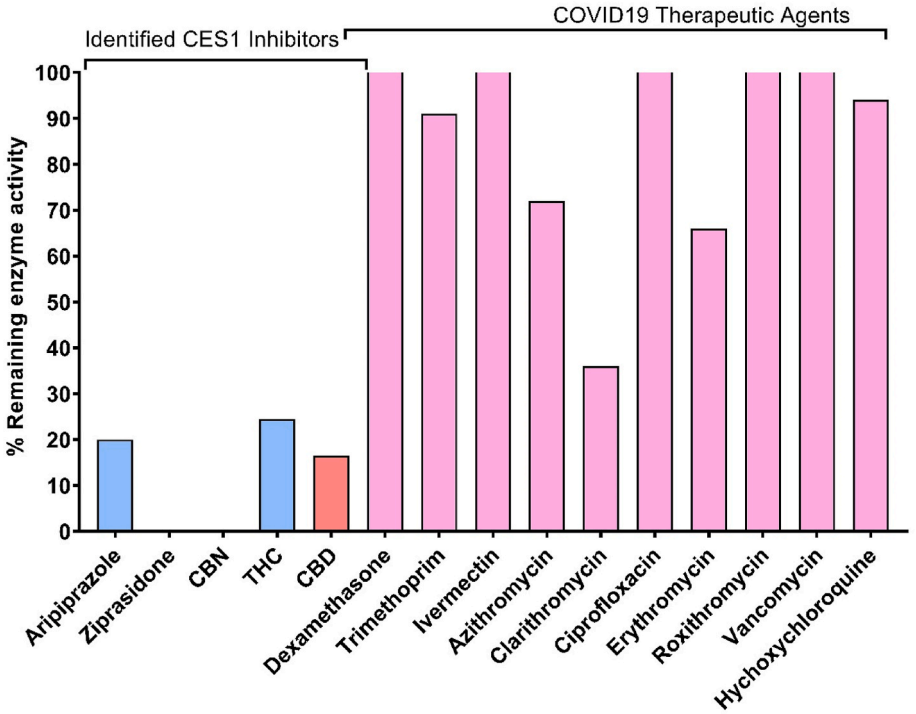

Fig. 4. In vitro coincubation of the COVID-19 therapeutic agents. The coadministration drug's final concentration is 10 μg/mL. Among all compounds assessed, CBD produced the strongest inhibition of RDV hydrolysis at 10 μg/mL.

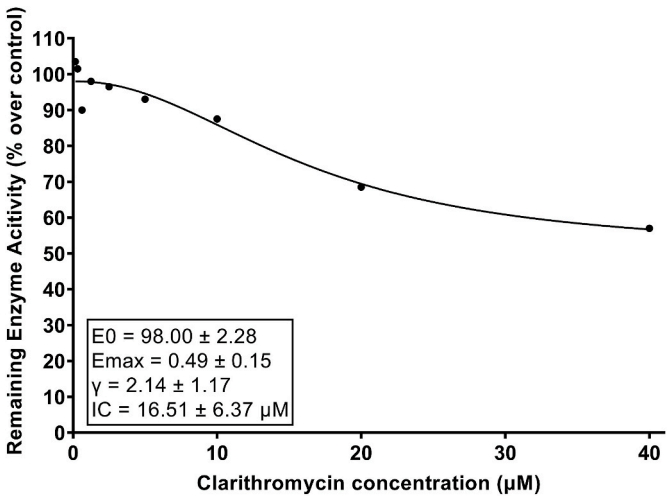

Fig. 5. Clarithromycin weakly inhibits RDV hydrolysis. Eq. (2) was used for regression. $r^2 = 0.94$.

3.5. CBD inhibited RDV hydrolysis via a mixed type-partial mechanism

To further investigate the mechanism of inhibition, we coincubated a series of concentrations of RDV with various concentrations of CBD. The results indicated that CBD inhibits RDV metabolism via a mixed type of competitive and noncompetitive partial inhibition. The inhibition type was closer to being characterized as a competitive inhibition ($\alpha = 1.05$), and the inhibition constant Ki = 0.89 μM. When binding with CBD, CES1 reduced the catalyzing efficiency to 24% ($\beta = 0.24$) (Fig. 7).

3.6. The CES1 G143E variant has 14% intrinsic clearance of that of wild-type

One extra concentration (500 μM) was added to the G143E group to evaluate maximum velocity. The in vitro evaluation shows the intrinsic clearance (Vmax/Km) in the presence of the *CES1* G143E variant is 14% of wild type CES1 on RDV metabolism (Fig. 8).

3.7. In vitro to in vivo scaling of clearance and AUC difference for RDV coadministration with CBD and CES1 G143E carrier and noncarrier

The result of in vitro to in vivo scaling was listed in Table 2. We predicted a potential decrease in clearance and an increase in AUC of RDV in coadministration with CBD over administration of RDV alone. We also predicted a potential decrease in clearance and an increase in AUC of RDV in G143E carrier subjects over non-carrier subjects.

4. Discussion

Intravenous RDV has been routinely utilized in the treatment of mild to moderate COVID-19 in high-risk, nonhospitalized patients and in hospitalized patients with COVID-19. An assessment of nine therapeutic agents frequently prescribed and often coadministered with RDV failed to produce significant inhibition of RDV hydrolysis. Clarithromycin shows a weak inhibition on RDV hydrolysis in our IC50 study (IC50 unable to be calculated). The lower residual enzyme activity in the screening results could be due to the simultaneous degradation of the substrate during the incubation. Nevertheless, considering the C_{max} attained in healthy subjects (2.85 μg/mL, 3.81 μM, Table 1) receiving clinically relevant doses, it would appear unlikely to produce a significant inhibitory effect [26]. However, consistent with previous in vitro studies employing other substrates, CBD produced potent inhibition of CES1-catalyzed hydrolysis [12]. The in vitro catalyzation velocity reduction in the presence of the *CES1* G143E variant was also identical

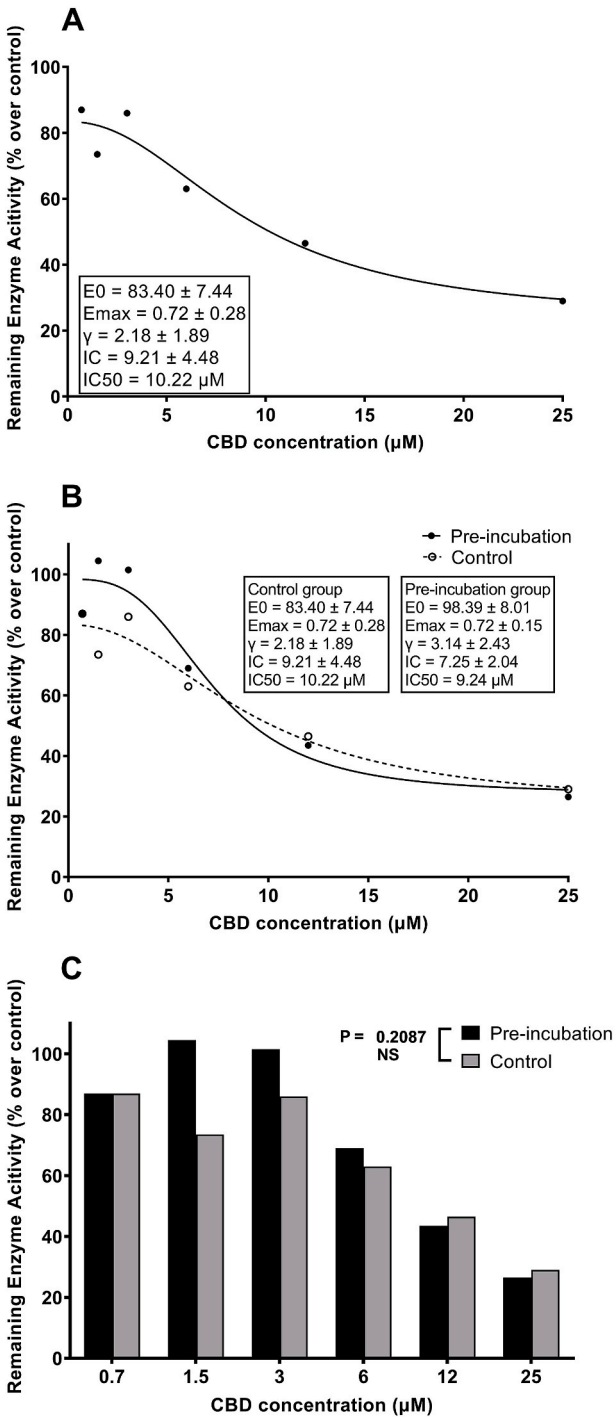

Fig. 6. IC50 of CBD-associated RDV hydrolysis and determination of the inhibition type. **Panel A:** IC50 of CBD vs RDV. Eq. (2) was used for regression. $r^2 = 0.94$. **Panel B:** determination of the inhibition type. A paired *t*-test was utilized to compare the preincubation group and control group. Control group $r^2 = 0.94$; Pre-incubation group $r^2 = 0.95$. **Panel C:** paired *t*-test of control group vs preincubation group, P = 0.21 (nonsignificant). Each data point was the average of the duplicate determinations. Values are shown with best fit value ± SE.

to our previous report [41].

The likelihood of CBD-RDV concurrent use and an attendant DDI liability is a possibility given the long elimination half-life of CBD and the interest in and promotion of CBD to treat COVID-19 and related conditions. For example, following in vitro study results suggesting the potential activity of CBD in reducing coronavirus replication and virus-

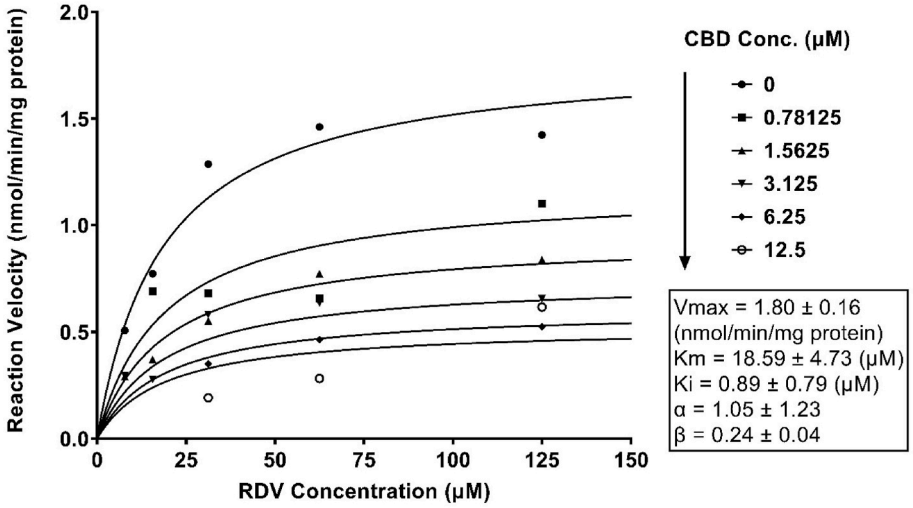

Fig. 7. Mechanism of CBD inhibiting RDV hydrolysis. Model: Eq. (4). $r^2 = 0.85$. Each data point represented the average of duplication. Values are shown with best fit value ± SE.

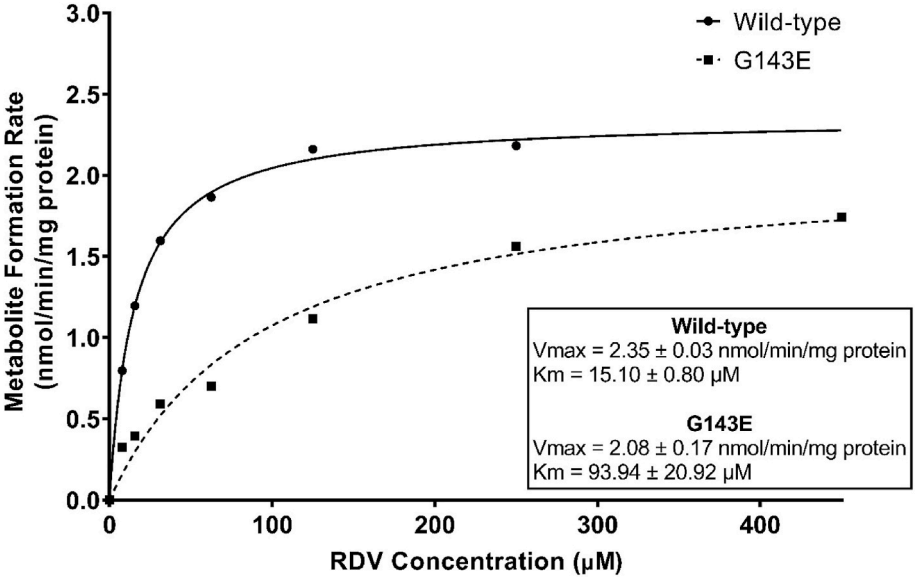

Fig. 8. S9 fraction incubation for RDV hydrolysis with *CES1* G143E. r^2 for the wild-type condition is > 0.99, r^2 for G143E is 0.97. Each data point was the mean of the duplicate time points. Values are shown with best fit value ± SE.

Table 2
In vitro to clinical scaling of CL and AUC change of co-administration of CBD and G143E polymorphism.

Coadministration with CBD					
Input Parameter	fm	α	β	Ki (μM)	[I] (μM)
Best fit value	0.91	1.05	0.24	0.89	4.40
SE	–	1.23	0.04	0.79	–
Reference	[3]	Experimental	Experimental	Experimental	[20]
Scaling Result	$CL_{int,I}/CL_{int,o}$	R_{CL}	R_{AUC}		
	0.36	0.42	2.40		
Genetic polymorphism					
Input Parameter	fm	$Vmax_{wt}$ (nmol/min/mg protein)	Km_{wt} (μM)	$Vmax_{G143E}$ (nmol/min/mg protein)	Km_{G143E} (μM)
Best fit value	0.91	2.35	15.10	2.08	93.94
SE	–	0.03	0.80	0.17	20.92
Reference	[3]	Experimental	Experimental	Experimental	Experimental
Scaling Result	$CL_{int,I}$ (mL/min/mg protein)	$CL_{int,o}$ (mL/min/mg protein)	$CL_{int,I}/CL_{int,o}$	R_{CL}	R_{AUC}
	0.02	0.16	0.14	0.22	4.56

induced cytokine release [10,42], CBD was recently approved by the FDA for a clinical trial to treat lung inflammation induced by COVID-19 [43] (Clinical trial identifier: NCT04686539, NCT04731116). In addition to our present evaluation, recent research from another group using microsomal incubations demonstrated that CBD inhibited RDV hydrolysis [44]. The potential DDI between CBD and the COVID-19 therapeutic agent RDV should be appreciated by clinicians using the antiviral. As our results (Table 1) suggested, when coadministered with CBD, the intrinsic clearance of RDV could likely be reduced – by as much as 36% (compared with using the same dose of RDV only). Additionally, the total clearance of RDV will be reduced to 42% of the value without CBD, and the AUC will be increased to 2.4-fold, compared with a condition of no coadministration with CBD.

There has been considerable interest in the potential role of pharmacogenomics in outcomes associated with COVID-19 therapeutics [45,46]. The *CES1* G143E variant was reported to have a clinical impact on several drugs that are CES1 substrates [47]. As a relatively new identified variant of a less well-studied DME with a lower MAF, the G143E polymorphism is not included on most of the commercial gene chips utilized in clinical genotyping efforts. For these potential reasons and others, the potential clinical implications (if any) of G143E carrier status in RDV-treated patients remains unknown. To our knowledge, our experiment is the first evaluation of the impact of the G143E variant in RDV hydrolysis through an in vitro approach. Notwithstanding the significant limitations of in vitro assessments and extrapolation of results to patients, our findings suggest that carriers of the G143E polymorphism might experience a significant reduction in the intrinsic clearance of RDV compared to non-carriers. According to FDA criteria for in vitro evaluation of DDIs, R_{AUC} greater than 1.02 may be considered to potentially produce a significant DDI (https://www.fda.gov/regulatory-information/search-fda-guidance-documents/invitro-drug-interaction-studies-cytochrome-p450-enzyme-and-transporter-mediated-drug-interactions). Our results suggested the intrinsic clearance of RDV could potentially be reduced to as much as 14% of the non-carriers. The total clearance of RDV was estimated to be reduced to 22% of the non-carriers, and the AUC was predicted to be increased to 4.6-fold compared with the non-carriers.

For RDV, which demonstrates significant antiviral efficacy against SARS-CoV-2 in vitro [48], it has lacked a robust clinical performance with variable outcomes and multiple associated toxicities [49]. Common side effects of RDV include nausea, vomiting, diarrhea, and elevation of hepatic enzymes ALT and AST [50]. More serious and potentially fatal side effects including bradycardia [51] and renal failure [52] have been reported. Currently, there is no clinical data regarding the potential for a DDI with RDV due to the CES1 inhibition, but the potential for a DDI mediated by CES1 inhibition has been noted in the literature [53]. The full toxicology of RDV remains incompletely understood and continues to be investigated. Recent in vitro research suggested that GS-704277 may be the critical mediator leading to nephrotoxicity [54]. Since the metabolism of RDV is sequential, the role of CES1 inhibition and changes in the dynamic plasma concentration change of GS-704277 and GS-441524 remains a matter of speculation, as well as any relationship to RDV efficacy and toxicity.

The results of the present in vitro evaluations assessing the potential CES1-mediated DDI potential between RDV and at least nine medications that have been commonly coadministered with the antiviral appear to be unlikely. However, there are a number of limitations to our research. First, our in vitro experiment was only designed to assess the hydrolysis and inhibition of hydrolysis mediated by CES1. Previous reports have indicated that beyond CES1, the enzyme CatA was also able to catalyze RDV hydrolysis [55]. It has been shown that the expression of CES1 and CatA is different across organ types [56], thus, the major contributing hydrolytic enzyme may differ across tissues [55]. Secondly, clinical studies have indicated that there is a significant systemic exposure to the CBD metabolites 6-OH-CBD, 7-OH-CBD, and 7-COOH-CBD after the administration of CBD [20]. The potential influences of these metabolites were not evaluated in this study. Additionally, the CES1/CatA expression pattern in the CES1-overexpressing HEK293 cells utilized in our assay may be substantially different from the organs of interest (e.g. liver vs lung) [13]. These potential differences may influence the accuracy of the in vitro to in vivo scaling model. Also, though the majority of RDV is biotransformed by hydrolysis, RDV is also a known substrate of several CYP enzymes including CYP2C8, CYP2D6, and CYP3A4 [57,58]. Several of the antibiotics screened in this study are also recognized as CYP inhibitors [8,59]. Notably, erythromycin, clarithromycin, and roxithromycin are known to be time-dependent inhibitors of CYP3A [60,61]. Although no appreciable effect on CES1-mediated RDV hydrolysis was demonstrated in our study, a potential DDI otherwise mediated by the CYP system was not evaluated. Finally, the influence of the assessed compounds on enzymes catalyzing the biotransformation of GS-704277 to GS-441524, and the further downstream biotransformation were not evaluated in these studies. As we mentioned in the introduction section, the further cascade activations involve multiple intracellular enzymes including a number of phosphoramides and phosphotransferases [55]. The quantitative distribution of the intermedia metabolic enzymes catalyzing RDV biotransformation in each step has not been studied clearly. With an in vitro enzyme or microsomal incubation system, it is hard to further metabolize GS-704277 to the final active form, thus a study in hepatocytes may need to be performed to estimate how CES1 inhibition could affect the formation of the final active metabolite GS-443902. Nonetheless, the results of these in vitro-in vivo predictions are of potential clinical concern. However, a clinical study designed to assess this suspected DDI would be required to confirm the prediction.

5. Conclusion

The results of the present in vitro evaluations assessing the potential CES1-mediated DDI potential between RDV and nine medications (hydroxychloroquine, ivermectin, erythromycin, clarithromycin, roxithromycin, trimethoprim, ciprofloxacin, vancomycin, and dexamethasone) commonly coadministered with the antiviral find no evidence for a likely interaction. On the other hand, the identified CES1 inhibitor aripiprazole and ziprasidone, as well as the major cannabinoids CBD, CBN, and THC, inhibited RDV metabolism by CES1. Cannabidiol inhibits RDV metabolism by a mixed type of competitive and noncompetitive partial inhibition mechanism, with $a = 1.05$, $Ki = 0.89$ μM. When binding with CBD, CES1 reduces the catalyzing capacity to 24% of the nonbinding enzyme. The intrinsic clearance (Vmax/Km) of the G143E carrier is 14% compared with the wild-type. In vitro to in vivo mathematical scaling predicted a potential 42% reduction in total clearance of RDV and potential 2.4-fold increase in RDV AUC when coadministered CBD. Predictive scaling also suggested a potentially 22% lower total clearance, and potential 4.6-fold higher AUC among G143E carriers. Our research was only designed to evaluate CES1-mediated RDV metabolism but biotransformation catalyzed by other enzymes were not evaluated. Further research needs to be performed to evaluate polymorphism any potential changes in RDV efficacy and potential toxicity secondary to CES1 inhibition. The coadministration of RDV with CBD or its use in patients carrying the G143E variant should be approached with caution due to the potential of impaired activation and clearance of RDV.

Author contributions

Study design: Q.Z., J.S.M.
Experimental design: Q.Z., J.S.M., P.W.M.
Analysis of data: Q.Z.
Preparation of the manuscript: Q.Z., J.S.M., P.W.M.

Declaration of competing interest

The authors declare that they have no known competing financial

interests or personal relationships that could have appeared to influence the work reported in this paper.

Data availability

Data will be made available on request.

Acknowledgments

This work was partially supported by the Eunice Kennedy Shriver National Institute of Child Health and Human Development [R01 HD093612].

References

[1] M.L. Agostini, E.L. Andres, A.C. Sims, R.L. Graham, T.P. Sheahan, X. Lu, E.C. Smith, J.B. Case, J.Y. Feng, R. Jordan, A.S. Ray, T. Cihlar, D. Siegel, R.L. Mackman, M. O. Clarke, R.S. Baric, M.R. Denison, Coronavirus susceptibility to the antiviral remdesivir (GS-5734) is mediated by the viral polymerase and the proofreading exoribonuclease, mBio 9 (2) (2018), https://doi.org/10.1128/mBio.00221-18.

[2] H.X.J. Lin, S. Cho, V. Meyyur Aravamudan, H.Y. Sanda, R. Palraj, J.S. Molton, I. Venkatachalam, Remdesivir in Coronavirus Disease 2019 (COVID-19) treatment: a review of evidence, Infection 49 (2021) 401–410, https://doi.org/10.1007/s15010-020-01557-7.

[3] R. Humeniuk, A. Mathias, H. Cao, A. Osinusi, G. Shen, E. Chng, J. Ling, A. Vu, P. German, Safety, tolerability, and pharmacokinetics of remdesivir, an antiviral for treatment of COVID-19, in healthy subjects, Clin. Transl. Sci. 13 (2020) 896–906, https://doi.org/10.1111/cts.12840.

[4] R. Humeniuk, A. Mathias, B.J. Kirby, J.D. Lutz, H. Cao, A. Osinusi, D. Babusis, D. Porter, X. Wei, J. Ling, Y.S. Reddy, P. German, Pharmacokinetic, pharmacodynamic, and drug-interaction profile of remdesivir, a SARS-CoV-2 replication inhibitor, Clin. Pharmacokinet. 60 (2021) 569–583, https://doi.org/10.1007/s40262-021-00984-5.

[5] Y. Pashaei, Analytical methods for the determination of remdesivir as a promising antiviral candidate drug for the COVID-19 pandemic, Drug Discov. Ther. 14 (2021) 273–281, https://doi.org/10.5582/ddt.2020.03097.

[6] O.A. Badary, Pharmacogenomics and COVID-19: clinical implications of human genome interactions with repurposed drugs, Pharmacogenomics J. 21 (2021) 275–284, https://doi.org/10.1038/s41397-021-00209-9.

[7] M. Yousefifard, A. Zali, A. Zarghi, A. Madani Neishaboori, M. Hosseini, S. Safari, Non-steroidal anti-inflammatory drugs in management of COVID-19; A systematic review on current evidence, Int. J. Clin. Pract. 74 (2020), e13557, https://doi.org/10.1111/ijcp.13557.

[8] B.S. Mayhew, D.R. Jones, S.D. Hall, An in vitro model for predicting in vivo inhibition of cytochrome P450 3A4 by metabolic intermediate complex formation, Drug Metab. Dispos. 28 (2000) 1031–1037.

[9] J.A. Rhoades, Y.K. Peterson, H.-J. Zhu, D.I. Appel, C.A. Peloquin, J.S. Markowitz, Prediction and in vitro evaluation of selected protease inhibitor antiviral drugs as inhibitors of carboxylesterase 1: a potential source of drug-drug interactions, Pharm. Res. (N. Y.) 29 (2012) 972–982, https://doi.org/10.1007/s11095-011-0637-9.

[10] J.H. Khalsa, G. Bunt, S.B. Maggirwar, S. Kottilil, COVID-19 and cannabidiol (CBD), J. Addiction Med. 15 (2021) 355–356, https://doi.org/10.1097/ADM.0000000000000771.

[11] B. Malinowska, M. Baranowska-Kuczko, A. Kicman, E. Schlicker, Opportunities, challenges and pitfalls of using cannabidiol as an adjuvant drug in COVID-19, Int. J. Mol. Sci. 22 (4) (2021), https://doi.org/10.3390/ijms22041986, 1986.

[12] Y. Qian, X. Wang, J.S. Markowitz, In vitro inhibition of carboxylesterase 1 by major cannabinoids and selected metabolites, Drug Metab. Dispos. 47 (2019) 465–472, https://doi.org/10.1124/dmd.118.086074.

[13] H.-J. Zhu, K.S. Patrick, H.-J. Yuan, J.-S. Wang, J.L. Donovan, C.L. DeVane, R. Malcolm, J.A. Johnson, G.L. Youngblood, D.H. Sweet, T.Y. Langaee, J. S. Markowitz, Two CES1 gene mutations lead to dysfunctional carboxylesterase 1 activity in man: clinical significance and molecular basis, Am. J. Hum. Genet. 82 (2008) 1241–1248, https://doi.org/10.1016/j.ajhg.2008.04.015.

[14] J.P. Lewis, R.B. Horenstein, K. Ryan, J.R. O'Connell, Q. Gibson, B.D. Mitchell, K. Tanner, S. Chai, K.P. Bliden, U.S. Tantry, C.J. Peer, W.D. Figg, S.D. Spencer, M. A. Pacanowski, P.A. Gurbel, A.R. Shuldiner, The functional G143E variant of carboxylesterase 1 is associated with increased clopidogrel active metabolite levels and greater clopidogrel response, Pharmacogenetics Genom. 23 (2013) 1–8, https://doi.org/10.1097/FPC.0b013e32835aa8a2.

[15] Z.-Y. Hu, A.N. Edginton, S.C. Laizure, R.B. Parker, Physiologically based pharmacokinetic modeling of impaired carboxylesterase-1 activity: effects on oseltamivir disposition, Clin. Pharmacokinet. 53 (2014) 825–836, https://doi.org/10.1007/s40262-014-0160-3.

[16] F. Zhang, H.-X. Li, T.-T. Zhang, Y. Xiong, H.-N. Wang, Z.-H. Lu, L. Xiong, Y.-Q. He, G.-B. Ge, Human carboxylesterase 1A plays a predominant role in the hydrolytic activation of remdesivir in humans, Chem. Biol. Interact. 351 (2021), https://doi.org/10.1016/j.cbi.2021.109744, 109744.

[17] D. Koller, S. Almenara, G. Mejía, M. Saiz-Rodríguez, P. Zubiaur, M. Román, D. Ochoa, M. Navares-Gómez, E. Santos-Molina, E. Pintos-Sánchez, F. Abad-Santos, Metabolic effects of aripiprazole and olanzapine multiple-dose treatment in a randomised crossover clinical trial in healthy volunteers: association with pharmacogenetics, Adv. Ther. 38 (2021) 1035–1054, https://doi.org/10.1007/s12325-020-01566-w.

[18] K.D. Wilner, R.A. Hansen, C.J. Folger, P. Geoffroy, The pharmacokinetics of ziprasidone in healthy volunteers treated with cimetidine or antacid, Br. J. Clin. Pharmacol. 49 (Suppl 1) (2000) 57S–60S, https://doi.org/10.1046/j.1365-2125.2000.00154.x.

[19] A. Gronewold, G. Skopp, A preliminary investigation on the distribution of cannabinoids in man, Forensic Sci. Int. 210 (2011) e7–e11, https://doi.org/10.1016/j.forsciint.2011.04.010.

[20] L. Taylor, B. Gidal, G. Blakey, B. Tayo, G. Morrison, A phase I, randomized, double-blind, placebo-controlled, single ascending dose, multiple dose, and food effect trial of the safety, tolerability and pharmacokinetics of highly purified cannabidiol in healthy subjects, CNS Drugs 32 (2018) 1053–1067, https://doi.org/10.1007/s40263-018-0578-5.

[21] Q. Bashir, M. Acosta, Comparative safety, bioavailability, and pharmacokinetics of oral dexamethasone, 4-mg and 20-mg tablets, in healthy volunteers under fasting and fed conditions: a randomized open-label, 3-way crossover study, Clin. Lymphoma, Myeloma & Leukemia 20 (2020) 768–773, https://doi.org/10.1016/j.clml.2020.06.022.

[22] S.A. Kaplan, R.E. Weinfeld, C.W. Abruzzo, K. McFaden, M.L. Jack, L. Weissman, Pharmacokinetic profile of trimethoprim-sulfamethoxazole in man, J. Infect. Dis. 128 (Suppl) (1973) 547–555, https://doi.org/10.1093/infdis/128.supplement_3.s547.

[23] A. González Canga, A.M. Sahagún Prieto, M.J. Diez Liébana, N. Fernández Martínez, M. Sierra Vega, J.J. García Vieitez, The pharmacokinetics and interactions of ivermectin in humans–a mini-review, AAPS J. 10 (2008) 42–46, https://doi.org/10.1208/s12248-007-9000-9.

[24] N.J. Lalak, D.L. Morris, Azithromycin clinical pharmacokinetics, Clin. Pharmacokinet. 25 (1993) 370–374, https://doi.org/10.2165/00003088-199325050-00003.

[25] G. Foulds, R.M. Shepard, R.B. Johnson, The pharmacokinetics of azithromycin in human serum and tissues, J. Antimicrob. Chemother. 25 (Suppl A) (1990) 73–82, https://doi.org/10.1093/jac/25.suppl_a.73.

[26] K.A. Rodvold, Clinical pharmacokinetics of clarithromycin, Clin. Pharmacokinet. 37 (1999) 385–398, https://doi.org/10.2165/00003088-199937050-00003.

[27] T. Bergan, A. Dalhoff, R. Rohwedder, Pharmacokinetics of ciprofloxacin, Infection 16 (Suppl 1) (1988) S3–S13, https://doi.org/10.1007/BF01650500.

[28] A.H.C. Chun, J.A. Seitz, Pharmacokinetics and biological availability of erythromycin, Infection 5 (1977) 14–22, https://doi.org/10.1007/BF01639131.

[29] H.B. Lassman, S.K. Puri, I. Ho, R. Sabo, M.J. Mezzino, Pharmacokinetics of roxithromycin (RU 965), J. Clin. Pharmacol. 28 (1988) 141–152, https://doi.org/10.1002/j.1552-4604.1988.tb05738.x.

[30] C.M. Bunke, G.R. Aronoff, M.E. Brier, R.S. Sloan, F.C. Luft, Vancomycin kinetics during continuous ambulatory peritoneal dialysis, Clin. Pharmacol. Ther. 34 (1983) 631–637, https://doi.org/10.1038/clpt.1983.225.

[31] M.R. Nicol, A. Joshi, M.L. Rizk, P.E. Sabato, R.M. Savic, D. Wesche, J.H. Zheng, J. Cook, Pharmacokinetics and pharmacological properties of chloroquine and hydroxychloroquine in the context of COVID-19 infection, Clin. Pharmacol. Ther. 108 (2020) 1135–1149, https://doi.org/10.1002/cpt.1993.

[32] M.M.A. Hamdy, M.M. Abdel Moneim, M.F. Kamal, Accelerated stability study of the ester prodrug remdesivir: recently FDA-approved Covid-19 antiviral using reversed-phase-HPLC with fluorimetric and diode array detection, Biomed. Chromatogr. 35 (2021), e5212, https://doi.org/10.1002/bmc.5212.

[33] I.H. Segel, Mixed-Type Inhibition, Enzyme Kinetics: Behavior and Analysis of Rapid Equilibrium and Steady-State Enzyme Systems, first ed., Wiley, Canada, 2014, pp. 170–202.

[34] L. Michaelis, M.L. Menten, K.A. Johnson, R.S. Goody, The original Michaelis constant: translation of the 1913 Michaelis-Menten paper, Biochemistry 50 (2011) 8264–8269, https://doi.org/10.1021/bi201284u.

[35] D.A. Volpe, S.S. Hamed, L.K. Zhang, Use of different parameters and equations for calculation of IC_{50} values in efflux assays: potential sources of variability in IC_{50} determination, AAPS J. 16 (2014) 172–180, https://doi.org/10.1208/s12248-013-9554-7.

[36] D.J. Greenblatt, Y. Zhao, K. Venkatakrishnan, S.X. Duan, J.S. Harmatz, S.J. Parent, M.H. Court, L.L. von Moltke, Mechanism of cytochrome P450-3A inhibition by ketoconazole, J. Pharm. Pharmacol. 63 (2011) 214–221, https://doi.org/10.1111/j.2042-7158.2010.01202.x.

[37] L.P. Volak, D.J. Greenblatt, L.L. von Moltke, In vitro approaches to anticipating clinical drug interactions, in: A.P. Li (Ed.), Drug–Drug Interactions in Pharmaceutical Development, John Wiley & Sons, Inc., Hoboken, NJ, USA, 2007, pp. 31–74, https://doi.org/10.1002/9780470187920.ch2.

[38] M. Rowland, S.B. Matin, Kinetics of drug-drug interactions, J. Pharmacokinet. Biopharm. 1 (1973) 553–567, https://doi.org/10.1007/BF01059791.

[39] Q. Zhang, S.X. Duan, J.S. Harmatz, Z. Wei, C.A. Singleton, D.J. Greenblatt, Mechanism of dasabuvir inhibition of acetaminophen glucuronidation, J. Pharm. Pharmacol. (2021) 131–138, https://doi.org/10.1093/jpp/rgab144.

[40] H.-J. Zhu, D.I. Appel, Y.K. Peterson, Z. Wang, J.S. Markowitz, Identification of selected therapeutic agents as inhibitors of carboxylesterase 1: potential sources of metabolic drug interactions, Toxicology 270 (2010) 59–65, https://doi.org/10.1016/j.tox.2010.01.009.

[41] H.-J. Zhu, J.S. Markowitz, Carboxylesterase 1 (CES1) genetic polymorphisms and oseltamivir activation, Eur. J. Clin. Pharmacol. 69 (2013) 733–734, https://doi.org/10.1007/s00228-012-1350-2.

[42] L.C. Nguyen, D. Yang, V. Nicolaescu, T.J. Best, T. Ohtsuki, S.-N. Chen, J.B. Friesen, N. Drayman, A. Mohamed, C. Dann, D. Silva, H. Gula, K.A. Jones, J.M. Millis, B.

C. Dickinson, S. Tay, S.A. Oakes, G.F. Pauli, D.O. Meltzer, G. Randall, M.R. Rosner, Cannabidiol inhibits SARS-CoV-2 replication and promotes the host innate immune response, BioRxiv [Preprint] (2021), https://doi.org/10.1101/2021.03.10.432967.

[43] J.A.S. Crippa, J.C. Pacheco, A.W. Zuardi, F.S. Guimarães, A.C. Campos, F. de L. Osório, S.R. Loureiro, R.G. Dos Santos, J.D.S. Souza, J.M. Ushirohira, R. R. Ferreira, K.C. Mancini Costa, D.S. Scomparin, F.F. Scarante, I. Pires-Dos-Santos, R. Mechoulam, F. Kapczinski, B.A.L. Fonseca, D.L.A. Esposito, A.D.C. Passos, J.E. C. Hallak, Cannabidiol for COVID-19 patients with mild to moderate symptoms (candidate study): a randomized, double-blind, placebo-controlled clinical trial, Cannabis Cannabinoid. Res. (2021), https://doi.org/10.1089/can.2021.0093.

[44] A. Saraswat, R. Vartak, M. Patki, K. Patel, Cannabidiol inhibits in vitro human liver microsomal metabolism of remdesivir: a promising adjuvant for COVID-19 treatment, Cannabis Cannabinoid. Res. (2021), https://doi.org/10.1089/can.2021.0109 [Epub ahead of print].

[45] B. Stanković, N. Kotur, V. Gašić, K. Klaassen, B. Ristivojević, M. Stojiljković, S. Pavlović, B. Zukić, Pharmacogenomics landscape of COVID-19 therapy response in Serbian population and comparison with worldwide populations, J. Med. Biochem. 39 (2020) 488–499, https://doi.org/10.5937/jomb0-26725.

[46] T. Takahashi, J.A. Luzum, M.R. Nicol, P.A. Jacobson, Pharmacogenomics of COVID-19 therapies, NPJ Genom. Med. 5 (2020) 35, https://doi.org/10.1038/s41525-020-00143-y.

[47] X. Wang, L. Her, J. Xiao, J. Shi, A.H. Wu, B.E. Bleske, H.-J. Zhu, Impact of carboxylesterase 1 genetic polymorphism on trandolapril activation in human liver and the pharmacokinetics and pharmacodynamics in healthy volunteers, Clin. Transl. Sci. 14 (2021) 1380–1389, https://doi.org/10.1111/cts.12989.

[48] S.C.J. Jorgensen, R. Kebriaei, L.D. Dresser, Remdesivir: review of pharmacology, pre-clinical data, and emerging clinical experience for COVID-19, Pharmacotherapy 40 (2020) 659–671, https://doi.org/10.1002/phar.2429.

[49] V.C. Yan, F.L. Muller, Why remdesivir failed: preclinical assumptions overestimate the clinical efficacy of remdesivir for COVID-19 and ebola, Antimicrob. Agents Chemother. 65 (2021), e0111721, https://doi.org/10.1128/AAC.01117-21.

[50] H.K. Elsawah, M.A. Elsokary, M.S. Abdallah, A.H. ElShafie, Efficacy and safety of remdesivir in hospitalized Covid-19 patients: systematic review and meta-analysis including network meta-analysis, Rev. Med. Virol. 31 (2021), e2187, https://doi.org/10.1002/rmv.2187.

[51] A. Touafchia, H. Bagheri, D. Carrié, G. Durrieu, A. Sommet, L. Chouchana, F. Montastruc, Serious bradycardia and remdesivir for coronavirus 2019 (COVID-19): a new safety concerns, Clin. Microbiol. Infect. (2021), https://doi.org/10.1016/j.cmi.2021.02.013 [Epub ahead of print].

[52] A.O. Gérard, A. Laurain, A. Fresse, N. Parassol, M. Muzzone, F. Rocher, V.L. M. Esnault, M.-D. Drici, Remdesivir and acute renal failure: a potential safety signal from disproportionality analysis of the WHO safety database, Clin. Pharmacol. Ther. 109 (2021) 1021–1024, https://doi.org/10.1002/cpt.2145.

[53] H. Rezaee, F. Pourkarim, S. Pourtaghi-Anvarian, T. Entezari-Maleki, T. Asvadi-Kermani, M. Nouri-Vaskeh, Drug-drug interactions with candidate medications used for COVID-19 treatment: an overview, Pharmacol. Res. Perspect. 9 (2021), e00705, https://doi.org/10.1002/prp2.705.

[54] V.C. Yan, F.L. Muller, Captisol and GS-704277, but not GS-441524, are credible mediators of remdesivir's nephrotoxicity, Antimicrob. Agents Chemother. 64 (2020), https://doi.org/10.1128/AAC.01920-20.

[55] R. Li, A. Liclican, Y. Xu, J. Pitts, C. Niu, J. Zhang, C. Kim, X. Zhao, D. Soohoo, D. Babusis, Q. Yue, B. Ma, B.P. Murray, R. Subramanian, X. Xie, J. Zou, J.P. Bilello, L. Li, B.E. Schultz, R. Sakowicz, J.Y. Feng, Key metabolic enzymes involved in remdesivir activation in human lung cells, Antimicrob. Agents Chemother. 65 (2021), e0060221, https://doi.org/10.1128/AAC.00602-21.

[56] L. Her, H.-J. Zhu, Carboxylesterase 1 and precision pharmacotherapy: pharmacogenetics and nongenetic regulators, Drug Metab. Dispos. 48 (2020) 230–244, https://doi.org/10.1124/dmd.119.089680.

[57] S. Deb, S. Arrighi, Potential effects of COVID-19 on cytochrome P450-mediated drug metabolism and disposition in infected patients, Eur. J. Drug Metab. Pharmacokinet. 46 (2021) 185–203, https://doi.org/10.1007/s13318-020-00668-8.

[58] K. Yang, What do we know about remdesivir drug interactions? Clin. Transl. Sci. 13 (2020) 842–844, https://doi.org/10.1111/cts.12815.

[59] A.A. Izzo, E. Ernst, Interactions between herbal medicines and prescribed drugs: an updated systematic review, Drugs 69 (2009) 1777–1798, https://doi.org/10.2165/11317010-000000000-00000.

[60] S. Zhou, S. Yung Chan, B. Cher Goh, E. Chan, W. Duan, M. Huang, H.L. McLeod, Mechanism-based inhibition of cytochrome P450 3A4 by therapeutic drugs, Clin. Pharmacokinet. 44 (2005) 279–304, https://doi.org/10.2165/00003088-200544030-00005.

[61] H. Yamazaki, T. Shimada, Comparative studies of in vitro inhibition of cytochrome P450 3A4-dependent testosterone 6beta-hydroxylation by roxithromycin and its metabolites, troleandomycin, and erythromycin, Drug Metab. Dispos. 26 (1998) 1053–1057.